Synthesis and Characterisation of a Very Low-Coordinate Diferrous [2Fe-2S] 0 Unit

Christian Schneider, Sophie Jana J Gross, Serhiy Demeshko, Sébastien Bontemps, Franc Meyer, Gunnar Werncke, C G Werncke

View Article Online
DOI: 10.1039/D1CC04196G

COMMUNICATION

Synthesis and Characterisation of a Very Low-Coordinate Diferrous [2Fe-2S]^0 Unit

C. Schneider,[a] S. J. Groß,[b] S. Demeshko,[b] S. Bontemps[c] F. Meyer,[b] C. G. Werncke[a]*

Received 00th January 20xx,
Accepted 00th January 20xx

DOI: 10.1039/x0xx00000x

Here we present the synthesis of a unique diferrous [2Fe–2S]^0 complex with only three-coordinate iron ions via reduction of a four-coordinate diferric [2Fe–2S]$^{2+}$ complex with concomitant ligand loss. The obtained compounds were thoroughly examined for their properties (e.g. by ^{57}Fe Mössbauer spectroscopy and magnetic susceptibility measurements). Facile cleavage of the [2Fe–2S] rhombus, commonly seen as rather stable, by CS_2 is also shown.

Iron sulphur units are an omnipresent structural motif in numerous metalloproteins such as ferredoxins, Rieske centres (**Figure 1**, **A**)[1,2] and bacterial nitrogenases (**Figure 1**, **B**)[3–5]. Their function ranges from electron transport, over small molecule activation, to sensing functions in different proteins.[6] In the last decade there has been an extensive development in the synthesis of molecular [2Fe–1S],[7,8] [2Fe–2S][9–13] and [4Fe–4S][14–17] clusters with mostly four-coordinate iron ions to contribute to the understanding of their reactivities and electronic structures.[18] Thereby, the impact of changes in the metal ions' oxidation state is of special interest. However, this is highly challenging on a synthetic level, especially for ligated, smaller Fe_2S_{1-2} units, which can be seen as essential elements of all higher nuclearity Fe/S clusters.[9] Furthermore, Fe/S clusters with low-coordinate iron sites are of particular interest for potential substrate activation, mostly inspired by the unique Fe–S–Fe belt units in the nitrogenase FeMo cofactor (**Figure 1**, **B**).[19]

Recently we reported the synthesis of a series of [2Fe–1S] complexes **D** (Figure 1) via reaction of elemental sulphur with the linear iron(I) complex $[FeL_2]^-$ (L = -N(Dipp)(SiMe$_3$)) and its subsequent, stepwise oxidation.[20] Despite their interesting electronic and magnetic features, the complexes were mostly inert towards nitrogenase relevant substrates which we attributed to the sterically demanding silylamide ligands.

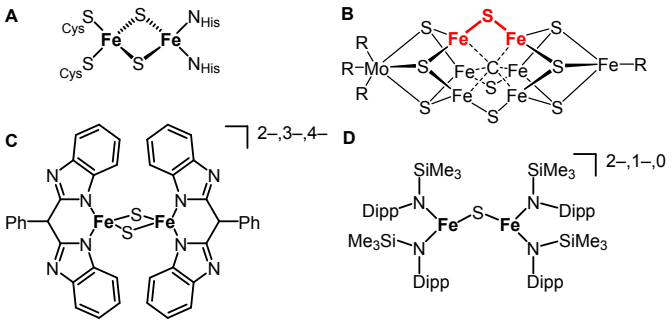

Figure 1. Central iron containing co-factor of the Rieske protein (**A**) and the nitrogenase (**B**) as well as examples of model compounds bearing different iron oxidation states (**C** and **D**).

Therefore, we were interested in using the sterically less demanding K{18c6}[Fe(N(SiMe$_3$)$_2$)$_2$] [**Fe^I**] (18c6 = 18-crown-6),[21] which was already shown as suitable platform for bond activation[22–24].

The reaction of a solution of [**Fe^I**] in Et_2O with 1/16 S_8 for 16 h led to a dark red solution, which afforded orange crystals upon storage at -30 °C for several days. X-ray diffraction analysis revealed the formation of the iron(II) *bis*-μ-sulphido complex K{18c6}[(Me$_3$Si)$_2$N)Fe(μ-S)]$_2$, **1**, (**Scheme 1, Figure 2**, left) instead of the envisioned mono-µ-sulphido complex.

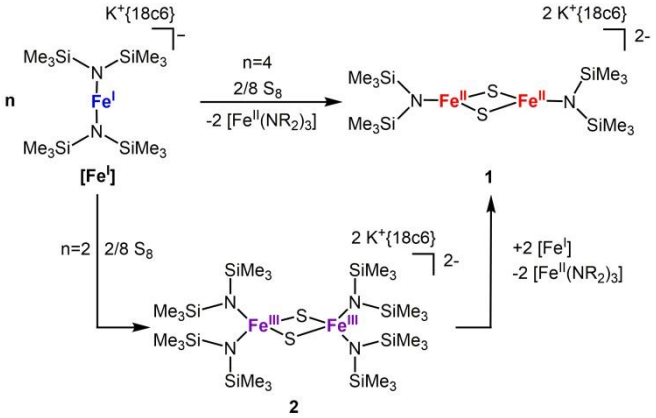

Scheme 1. Synthesis of complexes **1** and **2**.

[a] *Chemistry Department, Philipps-University, Hans-Meerwein-Str. 4, 35043 Marburg, Germany*
[b] *University of Göttingen, Institute of Inorganic Chemistry, Tammannstr. 4, D-37077 Göttingen, Germany.*
[c] *CNRS, LCC (Laboratoire de Chimie de Coordination), 205 route de Narbonne, 31077 Toulouse and Université de Toulouse, UPS, INPT, 31077 Toulouse, France.*

Electronic Supplementary Information (ESI) available: Experimental details, crystallographic details, SQUID, ^{57}Fe Mössbauer/UV/Vis/NMR data. See DOI: 10.1039/x0xx00000x

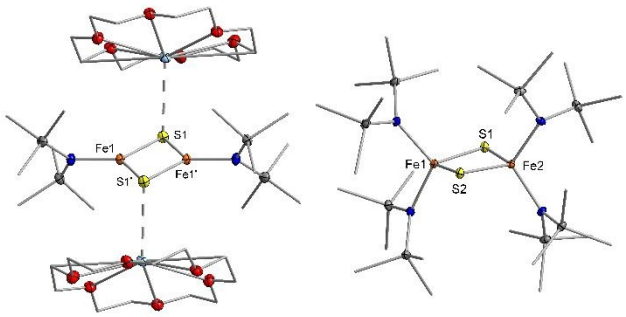

Figure 2. Molecular structures of **1** (left) and **2** (right) in the solid state. H atoms and the K^+(18c6) cations in structure **2** are omitted for clarity.

The [2Fe–2S] motif itself is well known in coordination and bioinorganic chemistry ([2Fe-2S] ferredoxins and Rieske-type clusters), where the iron ions are four coordinated. Few synthetic [2Fe–2S] clusters with five-coordinate metal ions are also known.[25] In contrast, **1** is a unique example of a [2Fe–2S] cluster with three-coordinate metal ions, each surrounded by two sulphido and one amido ligand. Accordingly, the core is found in an all-ferrous state, which is rarely achieved in case of [2Fe-2S] clusters.[10] Aside from **1** the known iron(I) trisamide K{18c6}[Fe(N($SiMe_3$)$_2$)$_3$] **[Fe^{II}(NR_2)$_3$]**[26] was found, which indicated that [**Fe^{I}**] acts not only as the reaction site but also as external reductant and amide scavenger. The formation of a bis-μ-sulphido compound instead of the envisioned monosulphido complex is likely due to the lowering of the steric demand of the silylamide -ligands and the stability of the [2Fe–2S] core. Insights into the formation of **1** was obtained by reacting [**Fe^{I}**] with equimolar amounts of sulphur. Upon storing the pentane layered reaction solution at -30 °C the iron(III) complex K{18c6}[(Me_3Si)$_2$N)$_2$Fe(μ-S)]$_2$, **2**, was isolated as a dark red crystalline solid (**Figure 2**, right) . When **2** was treated with two equivalents of [**Fe^{I}**] the reduced complex **1** was obtained.

The diferric bis(μ-sulphido) complex **2** features two tetrahedrally coordinated iron(III) ions (τ_4=0.97). The Fe–S distances (**Table 1**) of the [2Fe–2S] core are with 2.2235(5) – 2.2343(5) Å in line with other diferric [2Fe–2S] complexes.[9,11,15,27] In contrast, in **1** both iron ions of the [2Fe–2S] core are coordinated by only one additional amide ligand, which is an unprecedented structural motif. In addition, only a singular example of a structurally characterized fully reduced [2Fe–2S]^0 core was reported so far by some of us, using a dianionic, chelating amide ligand (**Figure 1**, **C**).[10] The coordination geometry around both three-coordinate iron ions in **1** is best described as Y-shaped (N–Fe–S 126.89° and 125.72°; S–Fe–S 107.83°). **2** experiences substantial structural changes of the [2Fe–2S] rhombus upon reduction to **1**. While we observe only a slight expansion of the Fe–S distance to 2.363 (5) Å, the Fe–Fe distance is reduced to 2.6494(5) Å, which is accompanied by contraction of the Fe–S–Fe angle from 79.491(2)° to 72.617(18)° and widening of the S–Fe–S angle from 99.813(2)° to 107.784(14). This behaviour is in contrast to previously reported series of isostructural [2Fe–2S]$^{2+,1+,0}$ complexes[11] with a virtually unchanged [2Fe–2S] core. For **1** the observed changes can be attributed in part to the loss of anionic amide ligands.

Table 1. Selected bond lengths (Å) and angles (°) of complexes **1** and **2**

View Article Online DOI: 10.1039/D1CC04196G

Compound	**1**	**2**
Fe–S	2.363(5)	2.2343(5)
Fe–Fe	2.6494(5)	2.8564(6)
Fe–N	1.9638(16)	2.0139(1)
Fe–S–Fe	72.617(18)	79.491(2)
S–Fe–S	107.784(14)	99.813(2)
N–Fe–S	126.89(5) 125.72(5)	110.78(4) 111.46(4)

Further, the acute angle Fe–S–Fe in **1** is likely caused by the Lewis acidic nature of the K^+18c6} cations. The relatively short K–S distance of 3.1430(6) Å is smaller than the sum of the van der Waals radii of both elements and points towards a significant contribution of the cation in the stabilization of the superreduced [2Fe–2S]^0 core. The beneficial role of the Lewis acidic K^+18c6} cation was also substantiated for the formation of **1** itself. Reaction of the K{crypt.222} derivative of [**Fe^{I}**] with S_8 gave **2** but did not effectuate subsequent reduction to **1**, which was also not possible using KC_8. As such we speculate that the reduction is intimately connected to the ligand dissociation, thus avoiding a highly negatively charged tetraligated [2Fe-2S] complex. The possible presence of a plausible mixed-valent/mixed-coordinate intermediate of the type [2Fe–2S]$^{1+}$ could not be substantiated, despite several attempts.

Based on the chemical reduction of **2** by [**Fe^{I}**] we investigated the electrochemical behaviour of **2** via cyclic voltammetry (supporting info). The cyclic voltammogram shows a quasireversible redox event at –1.8 V vs. Fc/Fc$^+$ (figure S5), which is the typical region for Fe$^{II/III}$ redox events of similar compounds.[9,11,15,28] The signal are broadened with high peak potential difference of 0.6 V, which indicates substantial structural changes, as evidenced via the formation of **1**. This observation, as well as the fact that there is just one broadened event instead of two well separate ones for each iron centre is in line with previous reports about the redox behaviour of [2Fe–2S] cores bearing monodentate anionic ligands.[15,28] Another interesting feature of the cyclic voltammogram of **2** is an irreversible oxidation (E = –0.7 V) only showing up after the oxidation at –1.53 V took place.

Complexes **1** and **2** were also characterized by zero-field ^{57}Fe Mössbauer spectroscopy. The Mössbauer spectrum of **2** shows a doublet with an isomer shift of δ = 0.35 mm/s and a quadrupole splitting of $|\Delta E_Q|$ = 0.60 mm/s (figure S7), clearly confirming the presence of four-coordinate, high-spin iron(III).[9,11] The isomer shift is higher than for the established β-ketiminato (δ = 0.29 mm/s, $|\Delta E_Q|$ = 1.06 mm/s)[9] and benzimidazolato[11] (δ = 0.24 mm/s, $|\Delta E_Q|$ = 0.87 mm/s) diferric [2Fe-2S] complexes, which we attribute to the π-donor character of the amido ligands as well as the slightly longer Fe–N and Fe–S bonds in case of **2**. The diferrous complex **1** shows a doublet with an isomer shift δ = 0.50 mm/s and a quadrupole splitting of $|\Delta E_Q|$ = 0.56 mm/s (Figure 3). To the best of our knowledge Mössbauer data for three coordinate iron(II)

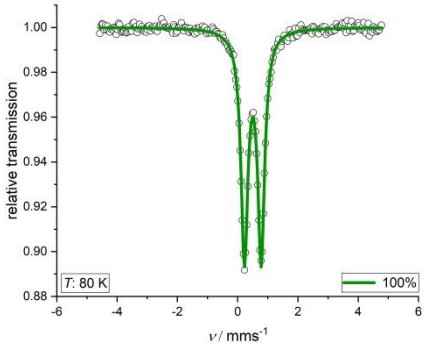

Figure 3. Mössbauer spectrum of **1** at 80 K. Parameters for **1**: δ = 0.50 mm/s, $|\Delta E_Q|$ = 0.56 mm/s.

featuring this specific coordination of two sulfides along with one amide ligand is absent in literature. However, it is in line with previously reported three coordinate high spin iron(II) complexes **$[Fe^{II}(NR_2)_3]^-$** (δ = 0.59 mm/s, $|\Delta E_Q|$ = 0.60 mm/s), $[Fe^{II}(S(Tripp))_3]^-$ (Tripp= 2,4,6-triisopropylphenyl) (δ = 0.57 mm/s, $|\Delta E_Q|$ = 0.81 mm/s), and the dianionic $[2Fe–1S]^{2+}$ complex **D** (δ = 0.59 mm/s, $|\Delta E_Q|$ = 0.22 mm/s) (**Figure 1**).[20,25,28] The isomer shift of a neutral *nacnac* based $[2Fe–1S]^{2+}$ complex is significantly higher (δ = 0.86 mm/s, $|\Delta E_Q|$ = 0.58 mm/s).[29]
Temperature dependent magnetic susceptibility measurements (SQUID) of **2** revealed an almost linear increase of χ_MT with temperature from 0.3 cm^3 K mol^{-1} at 70 K (S = 0 ground state) to 0.7 cm^3 K mol^{-1} at 295 K (figure S8), indicating strong antiferromagnetic coupling between the two iron(III) centers. The coupling constant J = –187 cm^{-1} is in line with previously reported all ferric [2Fe-2S] complexes (J = –179 cm^{-1} [11]; J = –209 cm^{-1} [9]) and was determined using $\hat{H} = -2J\hat{S}_A \cdot \hat{S}_B$ with $g_1 = g_2$ = 2.15. For **1** also a diamagnetic ground state (S = 0) is observed with a linear increase of $\chi_M T$ vs. the temperature from 0.06 cm^3Kmol^{-1} at 80 K to 0.17 cm^3Kmol^{-1} at 295 K (**Figure 4**). The curve is fit best with J = -348 cm^{-1} (g_1 = g_2 = 2). We tentatively attributed the larger J value of **1** to the substantially shorter Fe-Fe distance ($\Delta_{dFe–Fe}$ = –0.207 Å) with the added electrons in **1** residing in magnetically non-interacting d-orbitals.

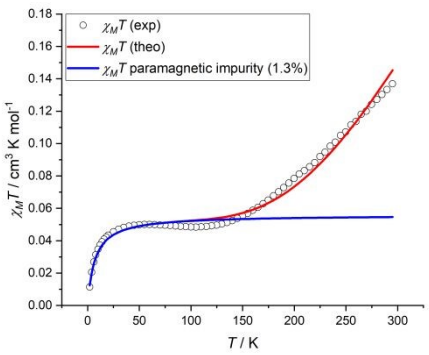

Figure 4 Variable-temperature magnetic susceptibility of solid **1** in the range 2–295 K (B = 0.5 T). The coupling constant J = –348 cm^{-1} was determined using $\hat{H} = -2J\hat{S}_A \cdot \hat{S}_B$ with g_1 = g_2 = 2.0 (fixed).

For diferrous Rieske clusters only weak antiferromagnetic coupling with J around –30 cm^{-1} was observed, and $-J \geq 40$ cm^{-1} was derived from ^{57}Fe Mössbauer spectra of a Cr^{II}-treated ferredoxin.[32] Similarly, for the previously reported type **C** diferrous [2Fe–2S] cluster $-J \geq 30$ cm^{-1} was estimated based on applied field Mössbauer data.[10] This stresses the unusual electronic structure of **1** with an exceptionally strong antiferromagnetic coupling between its three-coordinate iron ions, that is even significantly more pronounced than in complexes with shorter Fe–Fe distances for which metal-metal bonding is implied.[33–35] The ^{1}H-NMR spectrum of **1** shows a resonance at 3.50 ppm for the crown ether, as well as a broad paraagnetically shifted signal at -2.41 ppm ($w_{1/2}$ = 533.0 Hz) for the hmds ligand (**Figure S6**). **2** exhibits no resonance for the hmds ligands due to the even stronger paramagnetic nature of its Fe^{3+} ions (**Figure S7**). The UV-Vis spectrum of **1** shows a single band at 505 nm (ε = 1699 L/mol cm), while no distinct band beyond 400 nm is observed for **2** (**Figure S1**).
Recently, we observed the facile rupture of the central Fe–S unit by CS_2, a known competitive inhibitor of the FeMo-cofactor of the nitrogenase,[36–38] in a series of [2Fe–1S] complexes under thiocarbonate formation. As this behaviour was so far not reported on, we were curious if CS_2 might also break up a [2Fe–2S] motif. Indeed, reaction of **2** with an excess of CS_2 in THF led to the isolation of the thiocarbonato complex $K\{18c6\}[((Me_3Si)_2N)_2Fe(\eta^2\text{-}CS_3)]$ **3** (**Scheme 2**). In **3** the iron ion is coordinated by the two anionic silylamide ligands and a bidentate thiocarbonato ligand in a tetrahedral fashion.

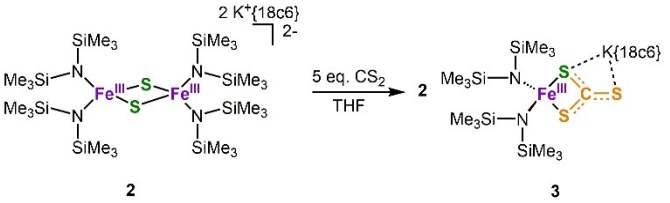

Scheme 2. Reaction of **2** with CS_2 to the thiocarbonate complex **3**.

We suppose that the K^+{18c6} cation plays a key role in the CS_2 activation. The flexible, monodentate amide ligands allow a Lewis acid base interaction between K^+ and a sulphide ligand similar to the one observed in the solid state structure of **1** (**Figure 2**). This would lead to elongation of the Fe–S bond followed by the insertion of the substrate and the rupture of the [2Fe–2S] core. The unique stabilizing role of K^+{18c6} became also obvious for the formation of **3** as analogous experiments with the crypt.222 derivative of **2** only led to decomposition. The result of the analogous reaction of **1** with CS_2 remained elusive to this date.
In conclusion, the reaction of $K\{18c6\}[Fe(N(SiMe_3)_2)_2]$ with elemental sulphur leads to the formation of the bis-μ-sulphido diferric complex **2**. The complex can be reduced further by $K\{18c6\}[Fe(N(SiMe_3)_2)_2]$ to the all ferrous form **1**, which uniquely features a $[2Fe–2S]^0$ core with only three-coordinate iron ions due to decoordination of amide ligands. Magnetic susceptibility measurements revealed sizeable antiferromagnetic coupling of the iron ions in both [2Fe–2S]

View Article Online
DOI: 10.1039/D1CC04196C

complexes, with an extraordinarily strong antiferromagnetic coupling (J = −348 cm^{-1}) for the reduced complex **1**. Reactivity studies of the diferrous complex **2** with CS_2 resulted in the surprising cleavage of the [2Fe–2S] unit, otherwise perceived as relatively robust, under thiocarbonate formation. In all these studies, the decisive role of the Lewis acidic K^+{18c8} counter ion, in transformation of the iron sulphur motif is revealed. Further analysis of the physical and chemical properties of **1** is under current scrutiny.

Acknowledgements

Funding by the Deutsche Forschungsgemeinschaft (DFG) is gratefully acknowledged: grants WE 5627/4-1 (to G. W.) and Me 1313/13-2 (to F.M. in the framework of the Priority Program SPP1927 “Iron Sulfur for Life”). S.B. thanks the CNRS for the facilities at LCC. L. Vendier is warmly acknowledged for initial X-Ray diffraction analyses as well as S. Sabo-Etienne for her support.

Conflicts of interest

There are no conflicts to declare.

Notes and references

1 E. I. Solomon, X. Xie and A. Dey, *Chem. Soc. Rev.*, 2008, **37**, 623–638.
2 D. Schneider and C. L. Schmidt, *Biochim. Biophys. Acta - Bioenerg.*, 2005, **1710**, 1–12.
3 T. Spatzal, J. Schlesier, E. M. Burger, D. Sippel, L. Zhang, S. L. A. Andrade, D. C. Rees and O. Einsle, *Nat. Commun.*, 2016, **7**, 10902.
4 J. A. Rees, R. Bjornsson, J. K. Kowalska, F. A. Lima, J. Schlesier, D. Sippel, T. Weyhermüller, O. Einsle, J. A. Kovacs and S. DeBeer, *Dalton Trans.*, 2017, **46**, 2445–2455.
5 T. Spatzal, M. Aksoyoglu, L. Zhang, S. L. A. Andrade, E. Schleicher, S. Weber, D. C. Rees and O. Einsle, *Science*, 2011, **334**, 940.
6 H. Beinert, R. H. Holm and E. Munck, *Science*, 1997, **277**, 653–659.
7 M. M. Rodriguez, B. D. Stubbert, C. C. Scarborough, W. W. Brennessel, E. Bill and P. L. Holland, *Angew. Chem. Int. Ed.*, 2012, **51**, 8247–8250.
8 D. E. DeRosha, N. A. Arnet, B. Q. Mercado and P. L. Holland, *Inorg. Chem.*, 2019, **58**, 8829–8834.
9 S. Yao, F. Meier, N. Lindenmaier, R. Rudolph, B. Blom, M. Adelhardt, J. Sutter, S. Mebs, M. Haumann, K. Meyer, M. Kaupp and M. Driess, *Angew. Chem. Int. Ed.*, 2015, **54**, 12506–12510.
10 A. Albers, S. Demeshko, K. Pröpper, S. Dechert, E. Bill and F. Meyer, *J. Am. Chem. Soc.*, 2013, **135**, 1704–1707.
11 A. Albers, S. Demeshko, S. Dechert, E. Bill, E. Bothe and F. Meyer, *Angew. Chem.*, 2011, **123**, 9357–9361.
12 J. Ballmann, A. Albers, S. Demeshko, S. Dechert, E. Bill, E. Bothe, U. Ryde and F. Meyer, *Angew. Chem. Int. Ed.*, 2008, **47**, 9537–9541.
13 A. Albers, S. Demeshko, S. Dechert, C. T. Saouma, J. M. Mayer and F. Meyer, *J. Am. Chem. Soc.*, 2014, **136**, 3946–3954.
14 C. R. Sharp, J. S. Duncan and S. C. Lee, *Inorg. Chem.*, 2010, **49**, 6697–6705.
15 K. Tanifuji, S. Tajima, Y. Ohki and K. Tatsumi, *Inorg. Chem.*, 2016, **55**, 4512–4518.
16 A. Sridharan, A. C. Brown and D. L. M. Suess, *Angew. Chem.*, 2021, **60**, 12802–12806.
17 Y. Ohki, Y. Sunada and K. Tatsumi, *Chem. Lett.*, 2005, **34**, 172–173.
18 S. Ohta and Y. Ohki, *Coord. Chem. Rev.*, 2017, **338**, 207–225.
19 D. E. DeRosha, V. G. Chilkuri, C. Van Stappen, E. Bill, B. Q. Mercado, S. DeBeer, F. Neese and P. L. Holland, *Nat. Chem.*, 2019, **11**, 1019–1025.
20 C. Schneider, S. Demeshko, F. Meyer and C. G. Werncke, *Chem. Eur. J.*, 2021, **27**, 6348–6353.
21 C. Gunnar Werncke, P. C. Bunting, C. Duhayon, J. R. Long, S. Bontemps and S. Sabo-Etienne, *Angew. Chem. Int. Ed.*, 2015, **54**, 245–248.
22 I. Müller and C. G. Werncke, *Chem. Eur. J.*, 2021, **27**, 4932–4938.
23 I. Müller, D. Munz and C. G. Werncke, *Inorg. Chem.*, 2020, **59**, 9521–9537.
24 I. Müller, C. Schneider, C. Pietzonka, F. Kraus and C. G. Werncke, *Inorganics*, 2019, **7**, 117.
25 M. G. G. Fuchs, S. Dechert, S. Demeshko, U. Ryde and F. Meyer, *Inorg. Chem.*, 2010, **49**, 5853–5858.
26 A. Eichhöfer, Y. Lan, V. Mereacre, T. Bodenstein and F. Weigend, *Inorg. Chem.*, 2014, **53**, 1962–1974.
27 P. Venkateswara Rao and R. H. Holm, *Chem. Rev.*, 2004, **104**, 527–559.
28 D. Coucouvanis, A. Salifoglou, M.G.Kanatzidis, A.Simopoulos and V.Papaefthymiou, *J. Am. Chem. Soc.*, 1984, **14**, 6081–6082.
29 F. M. Macdonnell, K. Ruhlandt-Senge, J. J. Ellison, R. H. Holm and P. P. Power, *Inorg. Chem.*, 1995, 1815–1822.
30 J. Vela, S. Stoian, C. J. Flaschenriem, E. Münck and P. L. Holland, *J. Am. Chem. Soc.*, 2004, **126**, 4522–4523.
31 E. J. Leggate, E. Bill, T. Essigke, G. M. Ullmann and J. Hirst, *PNAS*, 2004, **101**, 10913–10918.
32 S. J. Yoo, J. Meyer and E. Münck, *J. Am. Chem. Soc.*, 1999, **121**, 10450–10451.
33 L. Fohlmeister, S. Liu, C. Schulten, B. Moubaraki, A. Stasch, J. D. Cashion, K. S. Murray, L. Gagliardi and C. Jones, *Angew. Chem. Int. Ed.*, 2012, **51**, 8294–8298.
34 A. Klose, E. Solari, C. Floriani, A. Chiesi-Villa, C. Rizzoli and N. Re, *J. Am. Chem. Soc.*, 1994, **116**, 9123–9135.
35 R. A. Lewis, S. Morochnik, A. Chapovetsky, G. Wu and T. W. Hayton, *Angew. Chem. Int. Ed.*, 2012, **51**, 12772–12775.
36 L. C. Seefeldt, S. A. Ensign and M. E. Rasche, *Biochemistry*, 1995, **34**, 5382–5389.
37 M. E. Rasche and L. C. Seefeldt, *Biochemistry*, 1997, **36**, 8574–8585.
38 M. J. Ryle, H. I. Lee, L. C. Seefeldt and B. M. Hoffman, *Biochemistry*, 2000, **39**, 1114–1119.